

科学研究費助成事業 研究成果報告書

平成 29 年 9 月 26 日現在

機関番号：11301

研究種目：若手研究(B)

研究期間：2015～2016

課題番号：15K16318

研究課題名(和文) An Ultra-Sensitive and Ultra-Selective Electronic Nose System

研究課題名(英文) An Ultra-Sensitive and Ultra-Selective Electronic Nose System

研究代表者

Banan Ramin (Banan Sadeghian, Ramin)

東北大学・原子分子材料科学高等研究機構・助教

研究者番号：30728465

交付決定額(研究期間全体)：(直接経費) 2,900,000円

研究成果の概要(和文)：Si上の骨格筋組織の順応を成功裏に実証した後、我々は、1Hzの周波数および1-10msの持続時間を有するパルス電気刺激を適用することによって組織の機能性を調べた。パルスの振幅を変化させた。我々は、10または100μMの長さのマイクロプローブを含むSiチップ上にC2C12を開発した。予測されるように、筋管は、プローブ近傍で増強された筋形成をdemonstratingするマイクロプローブをうまく固定した。100μMのマイクロプローブを含むチップ上に形成された筋管は電気刺激に応答し、10μMのプローブには収縮せず、短いプローブが筋肉組織をしっかりと保持し、筋管収縮を妨げることが示された。

研究成果の概要(英文)：After successfully demonstrating the adherence of skeletal muscle tissue on Si, we examined the functionality of the tissue by applying pulsed electrical stimulation with a frequency of 1Hz, and duration of 1 - 10 ms. The amplitude of the pulse was varied. We showed that C2C12 myotubes are perfectly contractile on probeless Si wafers and quantified contraction scores. Later we developed C2C12 on the Si chips containing either 10 or 100 μM long microprobes terminated with sharp tips. As predicted, myotubes nicely anchored the microprobes demonstrating enhanced myogenesis at the vicinity of the probes. It was shown that myotubes formed on the chips containing 100 μM microprobes were responding to the electrical stimuli while those on the 10 μM probes did not contract suggesting that short probes firmly hold the muscle tissue and hinder myotube contraction.

研究分野：Electrical Engineering

キーワード：Biosensor Nanotechnology Nanowires

1. 研究開始当初の背景

The interfacing properties of vertically-aligned microwire or nanowire arrays with living cells have recently been under scrutiny by the bioengineering community. Substantial effort is being invested to develop nanostructures capable of interacting with cells individually or as tissues without impairing their viability. In this project I non-invasive interfacing of Si microprobes with skeletal muscle tissue.

2. 研究の目的

I have been studying the interfacing properties of Si microprobes, fabricated by vapor-solid-liquid (VLS) method. I showed that C2C12 cells cultured on the Si (111) microprobe substrates anchored preferentially to the microprobes, forming a whole cell layer. In addition, formation of myotube fibers (myogenesis) was enhanced at the microprobe trunks. These probes offer a huge potential in a variety of applications in medicine and tissue engineering such as localized piezoresistive motion detection, recording of action potentials, and extracellular biosensing. Following demonstration of excellent attachment, proliferation, and differentiation of muscle cells on Si substrates, I successfully induced contraction on the myotubes attached to the microprobes and measure the rates of superoxide generation from the contractile tissue in real-time. Chips containing microprobes with various lengths and pitches will be used in this project. They will be interfaced with the nanoporous gold based superoxide biosensors. The array of Si microprobes can be a suitable substitute for low resolution microelectrode arrays (MEA) and can simultaneously perform stimulation and sensing from cardiac and muscle tissue with high spatiotemporal resolution.

3. 研究の方法

3.1. Microembossing GelMA, cell seeding, and myogenesis. Polydimethylsiloxane (PDMS) stamps bearing the inverse pattern of the desired microgrooved GelMA templates were fabricated to host cells. GelMA itself in hydrogel form was made by mixing the prepolymer made in-house with a photoinitiator, all dissolved in Dulbecco's Phosphate-Buffered Saline at 65 C. 10 μ L

of the warm blend was dropped at the center of a 35 mm Petri dish and then the stamp was placed onto the mixture, defining a microgrooved area of 1 cm \times 1 cm. The ensemble was then exposed to UV light. Subsequently the stamp was removed carefully leaving behind the micropattern of crosslinked GelMA (Fig. 1a). The samples were kept soaked in PBS until cell seeding.

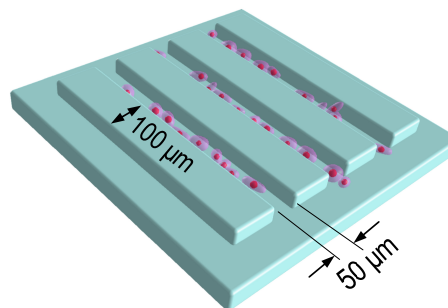


Fig. 1. Micropatterned GelMA containing C2C12 myoblasts

Murine C2C12 myoblasts were cultured in a medium composed of Dulbecco's Modified Eagle Medium (DMEM), 4-(2-hydroxyethyl)-1-piperazineethanesulfonic acid (HEPES), 1% penicillin-streptomycin (PS), and 10% fetal bovine serum. The myoblasts were trypsinized at \sim 70% confluency and seeded in 100 μ L aliquots containing 2×10^6 cells cm^{-3} cells onto the microgrooves. Samples were sterilized for 15 min (on each side of the membranes) on a clean bench under UV light, immediately before cell seeding. C2C12-carrying micropatterns were incubated so that the cells can settle, and then the medium was replenished. Fig. 2 shows merged phase-contrast and fluorescent images of the myoblasts, mostly entrapped and attached into the wells with a few residing on the wedges, at day 1 and day 2 of culture. After 4 days of culture, the growth medium was replaced with a differentiation medium based on DMEM with the addition of 20 mM HEPES, 1% PS, 2% horse serum as outlined earlier. Cells were retained therein for 4 days before conducting electrical stimulation. The differentiation medium was restored every 2 days.

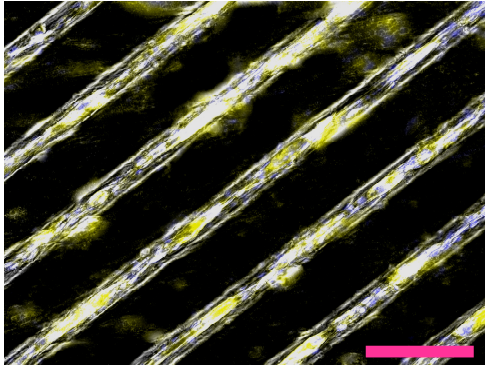


Fig. 2. Merged phase-contrast and fluorescent image of myoblasts formed in micropatterned GelMA. The scale bar is 100 μM .

3.2. Immunostaining, and visual quantification of myotube lengths
Myotubes were tagged at day 4 of differentiation using anti-fast skeletal myosin hooked to Alexa Fluor 488-conjugated anti-IgG and cell nuclei were revealed using 4,6-diamidino-2-phenylindole (DAPI). Multinucleated myotubes were located visually in the fluorescent images of immunostained samples (MY32+DAPI) snapped and recorded using AxioVision SE64 Rel. 4.9.1 software. Myotube lengths, defined as the longitudinal extent of myosin embedding three nucleus or more were measured using the same software. At least 100 myotubes were measured for each sample/condition.

3.3. Electrical stimulation setup and scheme, and signal processing.
Bipolar rectangular pulse (BRP) trains were generated using a commercial cell culture stimulator and applied to the electrochemical cells comprised of a 35 mm Petri dish base and two parallel platinum wires attached to the dish cap with a separation of 1.5 cm. The dish was filled with 2 mL of differentiation medium with the inclusion of, 1% MEM nonessential amino acid (100 \times), 2% MEM amino acid (50 \times), and 1 nM insulin. For overnight training, cell-carrying GelMA microgrooves were divided into three groups A, B, and C, and then subjected to BRP trains for 12 h, with a frequency of $f = 1$ Hz, pulse duration of $t_{\text{on}} = 0.5$ ms, and applied pulse amplitudes of $V_{\text{app}} = 3, 4, \text{ and } 4.5$ V, respectively.

For contractility analysis, one electrode was grounded and the signal was applied to the other through a 40 Ω shunt resistor to permit measurement of current and delivered energy. We fixed the pulse train

frequency at $f = 1$ Hz and swept V_{app} from 2 V to 5 V with $\Delta V = 0.5$ V intervals. The pulse on-time, t_{on} , was swept from 0.2 ms to 0.9 ms with $\Delta t_{\text{on}} = 0.1$ ms intervals, corresponding to a duty cycle range of 0.02% to 0.1%. Real-time movies ($f = 50$ frames per second) were captured for 23 seconds during excitation. Variations of pixel intensity over the area centered on the largest myotube nucleus were recorded using ImageJ utility (v.1.46r, NIH). The raw signal was then fed through a high-pass filter coded under Matlab to remove the DC component and low frequency noise, mainly caused by fluctuations in the stimulation medium. Figure 3 shows a typical filtered myotube contraction signal and the declaration of relevant parameters. We considered the full-width at half-maximum (FWHM) of the pulse, as the figure-of-merit for the response period. The response period, itself, is the sum of myotube contraction and relaxation times. Contraction scores were acquired by computing the standard deviation of the filtered signal.

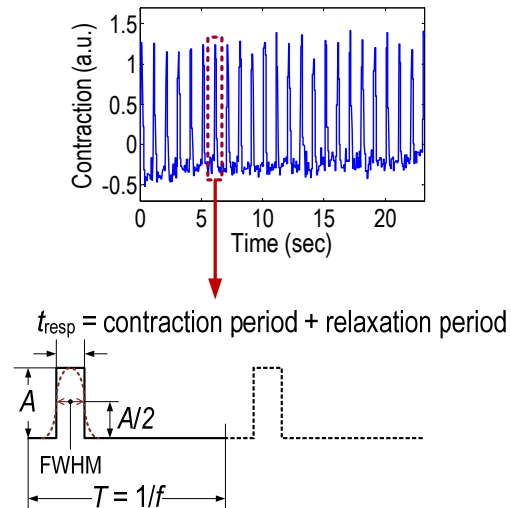


Fig. 3. Sample myotube response signal and the definition of relevant parameters.

V_{in} and V_{cell} are the instantaneous voltages at the power supply terminal and passed the shunt resistor, respectively, and I_{cell} is the current drawn by the electrochemical cell. A Randles equivalent circuit of the stimulation setup is illustrated in Fig. 4. V_{app} and R_s represent the open circuit output voltage and output impedance of the pulse wave generator, R_{elec} is the active electrolyte (stimulation medium) resistance, C_{dl} is the electrode double layer capacitance, and R_F represents the

resistance of the Faradaic reaction. The values of the equivalent circuit components and parameters were computed using the excitation voltage and current waveforms for a range V_{app} and t_{on} . Only R_{elec} is relatively invariant. Since the time constant of the electrochemical cell (τ_{cell}) is in the same order of magnitude as t_{on} , the applied waveform is only slightly altered at the electrode ends. The Randles circuit is helpful in explaining the dynamics of energy and charge transfer, their relation with the underlying contractility of myotubes, and later on, in computing the amount of current per myotube as a function of the total current drawn by the electrochemical cell.

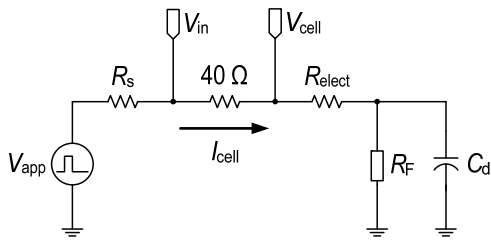


Fig. 4. Randles equivalent circuit for the stimulation electrochemical cell.

The average pulse amplitude at the electrochemical cell terminals was computed by averaging V_{cell} , and the total delivered electrical energy was computed by integrating the electrical power both over t_{on} .

3.4. Quantitative reverse transcription polymerase chain reaction (qRT-PCR) experiments.

Using PureLink RNA Mini Kit, we extracted the RNA of C2C12 myotubes developed on microgrooved GelMA, after exposure to overnight electrical stimulation under three different pulse amplitudes. At the same time, the RNA of a non-electrically stimulated myotubes on microgrooved GelMA sample was also extracted. Genomic DNA contamination was eliminated using the Purelink DNase Kit. 20 ng of purified RNA was used as a template for each PCR. Using a SuperScript III Platinum SYBR Green One-Step qRT-PCR Kit, single-step qRT-PCR was performed in four replicas in a MyiQ2 two-color RT-PCR detector. Relative genes expression levels were quantified using a comparative method ($2^{-\Delta Ct}$). The Ct (cycle threshold) values of the genes of interest were normalized to the Ct value of a reference gene (GAPDH).

qRT-PCR analysis were repeated three times in this work.

3.5. Statistical analysis

Using independent Student's t-test algorithm under Origin Pro 9.0 (OriginLab Co., USA), the differences between two data sets were deemed statistically significant, if the resulting p values were less than 0.05, or as noted otherwise. To quantify the length of myotubes, at least 100 myotubes of each set were analyzed.

4. 研究成果

4.1. Interfacing C2C12 myotubes with Si microprobes.

We reported on the establishment of skeletal muscle cell cultures on Si microprobes grown by a VLS technique. Excellent cell attachment, proliferation, and differentiation of muscle cells on Si microwire arrays were observed. C2C12 myoblasts cultured on the Si (111) substrate, anchored preferentially to the trunk of the microwires and formed a whole cell layer. After the medium was switched from growth to differentiation, myogenesis was also observed. Electrical stimulation promoted maturation of these microwire-anchoring myotubes. These micro-scale probes are targeted to be employed both as piezoresistive motion sensors and electrochemical biosensors for the characterization of myotube contractility and detection of biochemicals. Fig. 5a shows a well-developed muscle tissue formed on the microwire array. The tissue firmly attaches to the trunk of Si microwires. Presence of myotubes was confirmed by immunostaining with anti-fast skeletal myosin antibody revealed by Alexa Fluor 488-conjugated anti-IgG antibody (light magenta in Fig. 5b). Fig. 5c shows an SEM micrograph of a single Si microwire covered by muscle tissue.

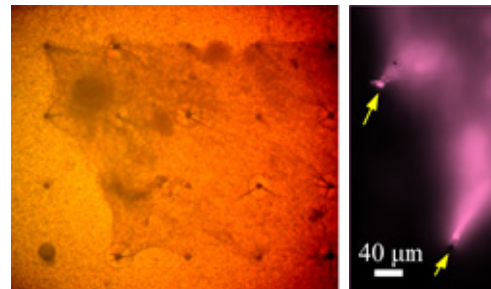


Fig. 5. (a) Phase contrast image of C2C12 tissue developed on the Si microwire array (spacing 200 μm), (b) Fluorescent image of immunostained myotubes anchoring two Si microprobes

4.2. Myotube electrical excitability and contractility.

C2C12 myotubes were first probed for electrical excitability at the end of day 4 of differentiation and then subjected to overnight electrical stimulation at three different voltages as explained earlier. Myotubes in the groves were more sensitive to electrical stimulus than those on the ridges, since they began to contract earlier as the excitation voltage or pulse duration were ramped up.

After overnight electrical stimulation, the contraction scores were recorded and organized based on t_{on} and I_{cell} . Fig. 6 shows the contraction profiles of representative myotubes from one set, both in time and frequency domains. These myotubes were excited under the I_{cell} and t_{on} pair that produced maximum contraction scores.

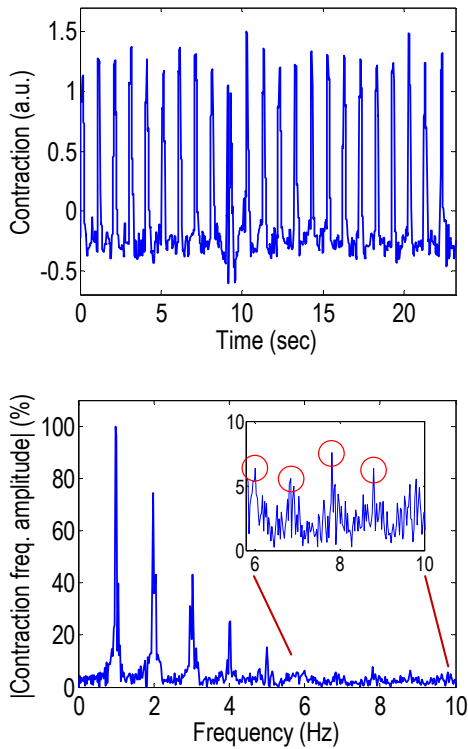


Fig. 6. Time domain (top row) and frequency domain (bottom row) high-pass filtered responses of representative trained C2C12 myotubes at maximum contractility, stimulated overnight under $V_{app} = 3$ V. The insets show magnifications of the frequency responses.

The average contraction scores for $n = 5$ contractile myotubes of each group are presented in the 3D matrix scatter plots of Fig. 7a. Rheobase and chronaxie values were estimated by applying non-linear

regression to the plots of I_{cell} vs. t_{on} at threshold. t_{on} at threshold is the minimum duration of the positive half of the pulse that could instigate contraction at a given pulse amplitude.

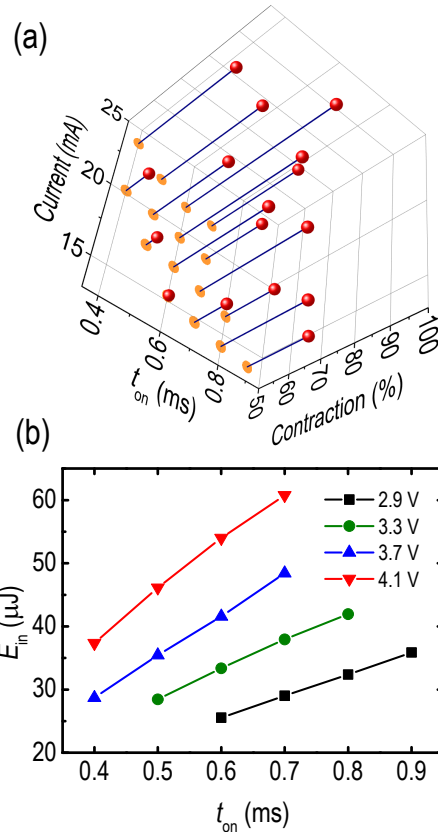


Fig. 7. Contraction and excitability data. (a) Contraction scores as a function of I_{cell} and t_{on} , normalized to the maximum value of the set (100 %). (b) Delivered electrical energy as a function of t_{on} for contractile myotubes, showing a linear dependence.

The graphs of Fig. 7b show the input electrical energy plotted as a function of t_{on} measured during post-training stimulation of contractile myotubes of each +ES group at four different V_{cell} values. They show that the electrical energy imposed to the tissue and required to instigate contraction (E_{in}), increases in a linear fashion with the pulse duration. The linear dependence of these two quantities is not trivial. At t_{on} (min), such required energy decreases as V_{cell} decreases, while a wider pulse is required to initiate contractility at a smaller E_{in} . We could thus infer a wider pulse would be favorable (to a certain extent) to trigger muscle contraction in our system, since it is accompanied not only by a smaller applied pulse amplitude but also demands less delivered energy.

We showed that overnight electrical stimulation at an adjusted pulse amplitude promotes maturation and contractility of aligned C2C12 myotubes formed in micropatterned hydrogel substrates. Analysis of the myotube instantaneous responses to BRP trains revealed that the myotubes exposed to the optimum pulse train condition display a repeatable contraction profile as a function of the excitation pulse amplitude and duration. Notably, these myotubes were grown longest, displayed the widest response pulse and the highest expression levels of maturation-related genes. Myotube contraction scores increase both with the excitation pulse amplitude and duty cycle to a certain extent. In addition, a larger pulse requires a shorter pulse duration to trigger myotube contraction.

5. 主な発表論文等

(研究代表者、研究分担者及び連携研究者には下線)

[雑誌論文] (計 4 件)

R. Banan Sadeghian, J. Han, S. Ostrovidov, S. Salehi, B. Bahraminejad, S. Ahadian, M. Chen, and A. Khademhosseini, "Macroporous Mesh of Nanoporous Gold in Electrochemical Monitoring of Superoxide Release from Skeletal Muscle Cells," *Biosensors and Bioelectronics*, Special Issue of Biosensors 2016, vol. **88**, pp. 41-47, 2017.

This paper was highlighted in the *AIMResearch* magazine, Dec. 2016 issue.

R. Banan Sadeghian, J. Han, J. Ribas, A. Nasajpour, M. Duchamp, S-A. Mousavi Shaegh, S. Ostrovidov, S. Salehi, M. Chen, and A. Khademhosseini, "Application of nanoporous gold in planar and mesh forms in electrochemical superoxide biosensing," in Proc. *IEEE Nano 2016*, pp. 19-21, Sendai, Japan, 22-25 Aug. 2016.

R. Banan Sadeghian, S. Ostrovidov, S. Salehi, J. Han, M. Chen, and A. Khademhosseini "An Electrochemical Biosensor based on Gold Microspheres and Nanoporous Gold for Real-time Detection of Superoxide Anion in Skeletal Muscle Tissue," in Proc. 37th *IEEE Engineering in Medicine and Biology Society (EMBS)*, pp. 7962-7965, Milan, Italy, 25-29 Aug. 2015.

R. Banan Sadeghian, Majid Ebrahimi, and Sahar Salehi "Electrical Stimulation of Microengineered Skeletal Muscle Tissue," Effect of Stimulus Parameters on Myotube Contractility and Maturation", *Journal of*

Tissue Engineering and Regenerative Medicine, doi: 10.1002/term.2502. [Epub ahead of print], 6/16/2017.

[学会発表] (計 4 件)

R. Banan Sadeghian, J. Han, M. Chen, and A. Khademhosseini, "Microporous Mesh of Mesoporous Gold, an Ultrasensitive Cell-based Electrochemical Biosensor," in Proc. *IEEE-EMBS - Micro and Nanotechnology in Medicine (MNM)*, Waikoloa, HI, 12-16 Dec. 2016.

R. Banan Sadeghian, J. Han, S. Ostrovidov, S. Salehi, M. Chen, and A. Khademhosseini, "A highly sensitive electrochemical biosensor based on three-dimensional network of nanoporous gold for online monitoring of superoxide release from skeletal muscle cells," *Biosensors 2016*, Gothenburg, Sweden, 25-27 May 2016.

R. Banan Sadeghian, "The Application of Metallic Glass Fibers in Future Hydrogel-based Scaffolds," *Energy Materials and Nanotechnology (ENM) Meeting on Metallic Glasses*, Kuala Lumpur, Malaysia, 12-16 Sept. 2016. (Invited Talk)

R. Banan Sadeghian, "Nanoporous Gold in 2D and 3D forms Applications in Ultrasensitive Electrochemical Superoxide Biosensing," 4th Annual Workshop on Micro- and Nanotechnologies for Medicine: Emerging Frontiers and Applications, Biomaterials Innovation Research Center, Cambridge MA, 25-29 Jul. 2016. (Invited Talk)

[その他]

ホームページ等

AIMResearch Highlight *Japanese* (Dec. 2016)

http://www.wpi-aimr.tohoku.ac.jp/jp/aimresearch/highlight/2017/20170130_000920.html

AIMResearch Highlight *English* (Dec. 2016)

http://www.wpi-aimr.tohoku.ac.jp/en/aimresearch/highlight/2016/20161226_000920.html

6. 研究組織

(1) 研究代表者

Ramin Banan Sadeghian

東北大学・原子分子材料科学高等研究機構・助教

研究者番号：30728465